

Zeeman-type spin splittings in strained d -wave altermagnets

Yahui Zhai,¹ Longju Yu,¹ Jian Lv,¹ Wei Zhang,¹ and Hong Jian Zhao^{1,2,3}

¹Key Laboratory of Material Simulation Methods and Software of Ministry of Education,
College of Physics, Jilin University, Changchun 130012, China

²Key Laboratory of Physics and Technology for Advanced Batteries (Ministry of Education),
College of Physics, Jilin University, Changchun 130012, China

³International Center of Future Science, Jilin University, Changchun 130012, China

(Dated: June 17, 2025)

Recently, altermagnetic materials have become rather attractive because such materials show-case combined advantages of ferromagnets (e.g., spin current) and antiferromagnets (e.g., low stray field and ultrafast spin dynamics). Symmetry arguments imply that d -wave altermagnets may host strain-induced nonrelativistic Zeeman-type spin splittings (ZSSs), but a theoretical, numerical, and experimental justification remains lacking. In the present work, we work with collinear spin point groups (SPGs) and use symmetry analysis to identify 15 SPGs that host strain-induced nonrelativistic ZSSs. These 15 SPGs coincide with the cases associated with d -wave altermagnetic spin splittings reported in literature. We further corroborate our analysis by first-principles numerical simulations, which indicate that a shear strain of 2% creates sizable nonrelativistic ZSSs of up to 177, 100, and 102 meV in CoF₂, LiFe₂F₆ and La₂O₃Mn₂Se₂ d -wave altermagnetic semiconductors, respectively. Our work suggests an alternative route toward creating spin current in altermagnets, which may be used to design altermagnetic-based spintronic devices.

I. INTRODUCTION

The creation of spin current is of particular importance in spintronics [1–4]. Conventional ferromagnets or canted antiferromagnets (with weak magnetization) host Zeeman-type spin splittings (ZSSs) [5–10], and therefore accommodate spin-polarized carriers and enable spin current [1, 4, 11, 12]. Unlike conventional ferromagnets or antiferromagnets, the recently discovered altermagnets exhibit various ferromagnetic-like phenomena such as broken Kramers degeneracy [13–21], the anomalous Hall/Nernst effect [22–27], giant/tunneling magnetoresistance effect [28–33]. Moreover, altermagnets also retain a variety of advantages of antiferromagnets (i.e., low stray fields and ultrafast spin dynamics [34–36]). Because of the combined advantages of ferromagnets and antiferromagnets, altermagnetic materials offer an innovative and unique platform for the development of future spintronic devices with high performance. Usually, altermagnetic materials are associated with d -, g -, or i -wave altermagnetic spin splittings [37], where d -wave (respectively, g -, or i -wave) spin splitting can be utilized to generate linear (respectively, nonlinear) spin current [38–44]. As shown in Ref. [37], the collinear altermagnetic materials with d -wave spin splittings can be attributed to 15 collinear spin point groups (SPGs). Generally, the d -wave altermagnetic spin splitting between two momentum directions is described by $\lambda_{\alpha\beta}k_{\alpha}k_{\beta}\sigma_{\chi}$ [37, 45], where k_{α} and k_{β} are wave vector components along α and β directions, and σ_{χ} is the Pauli matrix component along the χ direction. From symmetry point of view, $k_{\alpha}k_{\beta}$ transforms identically as the $\eta_{\alpha\beta}$ strain [46]. This implies that altermagnets with $\lambda_{\alpha\beta}k_{\alpha}k_{\beta}\sigma_{\chi}$ altermagnetic splittings naturally host strain-induced nonrelativistic Zeeman-type spin splittings (ZSSs) described by $\tilde{\lambda}_{\alpha\beta}\eta_{\alpha\beta}\sigma_{\chi}$. Nevertheless, a theoretical, numerical, and experimental jus-

tification of strain-induced nonrelativistic ZSSs in altermagnets remains lacking.

Focusing on d -wave altermagnetic materials, the present work aims at exploring the nonrelativistic ZSSs that are rooted in mechanical strain. We carry out a systematic symmetry analysis with respect to 58 collinear antiferromagnetic SPGs, and identify 15 SPGs that host strain-induced nonrelativistic ZSSs [coinciding with the aforementioned 15 cases associated with d -wave altermagnetic spin splittings (see Ref. [37])]. We also derive two-band effective models to describe altermagnetic spin splittings and strain-induced nonrelativistic ZSSs. We further numerically check our analysis regarding strain-induced ZSSs by working with three typical d -wave altermagnetic semiconductors (i.e., CoF₂, LiFe₂F₆ and La₂O₃Mn₂Se₂). By first-principles simulations, we find that shear strain η_{xy} creates nonrelativistic ZSSs in these three materials. Strikingly, a η_{xy} strain of 2% yields nonrelativistic ZSSs as giant as 177 meV in CoF₂, and creates sizable ZSSs of ~ 100 meV in LiFe₂F₆ and La₂O₃Mn₂Se₂.

II. METHODS

We performed first-principles simulations by using the Vienna Ab initio Simulation Package (VASP) [47, 48]. We first relaxed the crystal structures of CoF₂, LiFe₂F₆, and La₂O₃Mn₂Se₂ under various strains with the force convergence criterion of 5 meV/Å, and then computed the band structures for these systems. During our calculations, we adopted the PBEsol [49] exchange-correlation functional and Projector Augmented Wave (PAW) approach [50], without involving spin-orbit interaction. We used kinetic cutoff energies of 550 eV for CoF₂, 650 eV for LiFe₂F₆, and 550 eV for La₂O₃Mn₂Se₂, and solve the following electronic configurations: 3s²3p⁶3d⁸4s¹ for

Co, $2s^2 2p^5$ for F, $1s^2 2s^1$ for Li, $3s^2 3p^6 3d^7 4s^1$ for Fe, $5s^2 5p^6 5d^1 6s^2$ for La, $3s^2 3p^6 3d^6 4s^1$ for Mn, $2s^2 2p^4$ for O, and $4s^2 4p^4$ for Se. We considered the correlation effects by adding effective Hubbard U corrections (by the Dudarev approach[51]) of 3 eV, 4 eV and 4 eV to the $3d$ orbitals of Co, Fe and Mn, respectively, following Refs. [52–54]. We selected the k -point meshes of $8 \times 8 \times 11$ for CoF_2 , $8 \times 8 \times 4$ for LiFe_2F_6 and $6 \times 6 \times 2$ for $\text{La}_2\text{O}_3\text{Mn}_2\text{Se}_2$. We employed Vaspkit [55, 56], Vesta [57], Mathematica [58], Bilbao Crystallographic Server [59–61], Magndata [62–64], Pyprocar [65, 66], The Material Project [67], Find Spin Group [68] and Matplotlib [69] in the present work as well.

III. RESULTS AND DISCUSSION

Our results and discussion contain two subsections. In Section A, we analyze the symmetries of SPGs and derive the effective Hamiltonians that describe the alternating magnetic spin splittings and strain-induced ZSSs in altermagnets. In Section B, we use first-principles simulations to numerically verify our analysis, by working with CoF_2 , LiFe_2F_6 and $\text{La}_2\text{O}_3\text{Mn}_2\text{Se}_2$ altermagnetic semiconductors.

A. Effective Hamiltonians

In d -wave altermagnets, the momentum-resolved spin splittings (sketched in Fig. 1) are described by the two-band effective Hamiltonian [37, 45]

$$H_{\text{eff}}(\mathbf{k}) = \sum_{\alpha\beta} \lambda_{\alpha\beta} k_\alpha k_\beta \sigma_\chi, \quad (1)$$

where \mathbf{k} is the wave vector, k_α (k_β) the α (β) component of \mathbf{k} , σ_χ the Pauli matrix component along the χ direction. Here, we assume that the magnetic moments are aligned along $\pm\chi$ direction in a collinear way. As shown in Ref. [37], 15 SPGs host such d -wave altermagnetic spin splittings, and effective Hamiltonians associated with these SPGs are summarized in Table SI of the Supplementary Material of Ref. [37]. Because $k_\alpha k_\beta$ transforms identically as the mechanical strain $\eta_{\alpha\beta}$ under spatial and temporal symmetry operations [46], Eq. (1) can be generalized as

$$\tilde{H}_{\text{eff}}(\{\eta_{\alpha\beta}\}) = \sum_{\alpha\beta} \tilde{\lambda}_{\alpha\beta} \eta_{\alpha\beta} \sigma_\chi, \quad (2)$$

where the $\eta_{\alpha\beta}$ contains six independent strain tensor components (i.e., η_{xx} , η_{yy} , η_{zz} , η_{xy} , η_{yz} , and η_{xz}). Therefore, we conclude that d -wave altermagnets (SPGs listed in the aforementioned Table SI [37]) host strain-induced nonrelativistic ZSSs as well. In the following, we extract the SPGs associated with strain-induced nonrelativistic ZSSs, derive their corresponding effective Hamiltonians, and compare our results with Table SI of Ref. [37]. The

SPGs contain 90 collinear cases and 58 of them describe the symmetries of collinear antiferromagnets [68, 70–73]. We focus on the 58 collinear antiferromagnetic SPGs and derive the symmetry-adapted effective Hamiltonians for them.

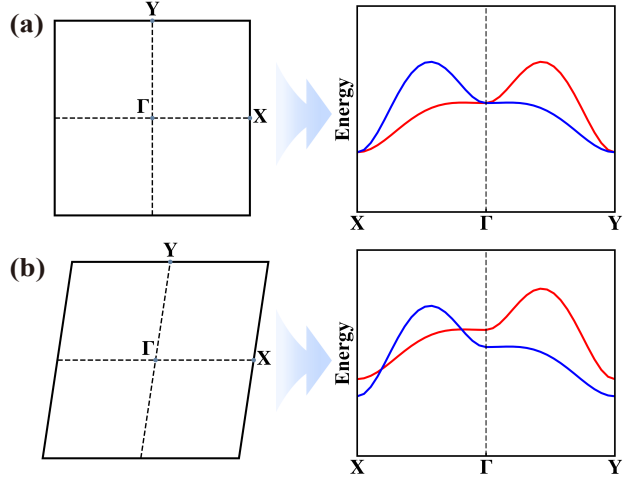


FIG. 1. Schematic illustrations of the Brillouin zones and band structures for a d -wave altermagnet with alternating spin splitting (a) and strain-induced nonrelativistic ZSSs (b). The spin-up and spin-down electronic states are colored in red and blue, respectively.

To begin with, we briefly introduce the collinear SPGs. We basically follow the conventions shown in Refs. [68, 70–73]. According to Refs. [68, 70–73], the symmetry operations in SPGs can be written as $[g_s||g_l]$, with g_s and g_l being symmetry operations in spin and spatial spaces, respectively. In particular, the $[g_s||g_l]$ operation transforms $\eta_{\alpha\beta}$ and σ_χ as $[g_s||g_l] : \eta_{\alpha\beta} \rightarrow g_l \eta_{\alpha\beta}$ and $[g_s||g_l] : \sigma_\chi \rightarrow g_s \sigma_\chi$. We recall that the SPGs (G_{sp}) are formulated as [68, 70–73]

$$G_{sp} = G_{so} \otimes G_{ns}. \quad (3)$$

Here, G_{so} is the so-called spin-only group and G_{ns} is known as the nontrivial spin point group [68, 70–73]. For

TABLE I. Transformation rules for $\eta_{\alpha\beta}$ strain and σ_χ Pauli matrix with respect to the nontrivial SPG (G_{ns}) for $14^\infty m 1$ SPG. Here, the symmetry operations in the spin space (left side of ‘||’) include identity operation (1) and time reversal operation (\mathcal{T}), while the symmetry operations in the spatial part (right side of ‘||’) contain identity operation (1), two-fold rotation along z -axis ($2_{\text{oo}1}$), and rotation of $\pm \frac{\pi}{4}$ along the z axis ($4_{\text{oo}1}^\pm$).

	η_{xx}	η_{yy}	η_{zz}	η_{xy}	η_{xz}	η_{yz}	σ_χ
$P_{[1 1]}$	η_{xx}	η_{yy}	η_{zz}	η_{xy}	η_{xz}	η_{yz}	σ_χ
$P_{[1 2_{\text{oo}1}]}$	η_{xx}	η_{yy}	η_{zz}	η_{xy}	$-\eta_{xz}$	$-\eta_{yz}$	σ_χ
$P_{[\mathcal{T} 4_{\text{oo}1}^+]}$	η_{yy}	η_{xx}	η_{zz}	$-\eta_{xy}$	η_{yz}	$-\eta_{xz}$	$-\sigma_\chi$
$P_{[\mathcal{T} 4_{\text{oo}1}^-]}$	η_{yy}	η_{xx}	η_{zz}	$-\eta_{xy}$	$-\eta_{yz}$	η_{xz}	$-\sigma_\chi$

TABLE II. The SPGs that are associated with the d -wave altermagnetism and host the strain-induced nonrelativistic ZSSs. The effective Hamiltonians describing the strain-induced nonrelativistic ZSSs and the alternating spin splittings are shown in the second and third columns, respectively. Note that, the effective Hamiltonians that has been derived in literature are endowed with a reference number after the corresponding formula.

SPGs	The effective Hamiltonian	The effective Hamiltonian
$\bar{1}m^{\infty}1$	$\tilde{\lambda}_{xy}\eta_{xy}\sigma_{\chi} + \tilde{\lambda}_{yz}\eta_{yz}\sigma_{\chi}$	$\lambda_{xy}k_xk_y\sigma_{\chi} + \lambda_{yz}k_yk_z\sigma_{\chi}$
$\bar{1}2^{\infty}1$	$\tilde{\lambda}_{xy}\eta_{xy}\sigma_{\chi} + \tilde{\lambda}_{yz}\eta_{yz}\sigma_{\chi}$	$\lambda_{xy}k_xk_y\sigma_{\chi} + \lambda_{yz}k_yk_z\sigma_{\chi}$
$\bar{1}2/\bar{1}m^{\infty}1$	$\tilde{\lambda}_{xy}\eta_{xy}\sigma_{\chi} + \tilde{\lambda}_{yz}\eta_{yz}\sigma_{\chi}$	$\lambda_{xy}k_xk_y\sigma_{\chi} + \lambda_{yz}k_yk_z\sigma_{\chi}$ [37, 45]
$\bar{1}2\bar{1}2^{\infty}1$	$\tilde{\lambda}_{xy}\eta_{xy}\sigma_{\chi}$	$\lambda_{xy}k_xk_y\sigma_{\chi}$
$\bar{1}m^{\bar{1}}m^12^{\infty}1$	$\tilde{\lambda}_{xy}\eta_{xy}\sigma_{\chi}$	$\lambda_{xy}k_xk_y\sigma_{\chi}$
$\bar{1}m^1m^{\bar{1}}2^{\infty}1$	$\tilde{\lambda}_{xz}\eta_{xz}\sigma_{\chi}$	$\lambda_{xz}k_xk_z\sigma_{\chi}$
$\bar{1}m^{\bar{1}}m^1m^{\infty}1$	$\tilde{\lambda}_{xy}\eta_{xy}\sigma_{\chi}$	$\lambda_{xy}k_xk_y\sigma_{\chi}$ [45]
$\bar{1}4^{\infty}1$	$\tilde{\lambda}_{xy}\eta_{xy}\sigma_{\chi} + \tilde{\lambda}_{xx}(\eta_{xx} - \eta_{yy})\sigma_{\chi}$	$\lambda_{xy}k_xk_y\sigma_{\chi} + \lambda_{xx}(k_xk_x - k_yk_y)\sigma_{\chi}$
$\bar{1}\bar{4}^{\infty}1$	$\tilde{\lambda}_{xy}\eta_{xy}\sigma_{\chi} + \tilde{\lambda}_{xx}(\eta_{xx} - \eta_{yy})\sigma_{\chi}$	$\lambda_{xy}k_xk_y\sigma_{\chi} + \lambda_{xx}(k_xk_x - k_yk_y)\sigma_{\chi}$
$\bar{1}4/1m^{\infty}1$	$\tilde{\lambda}_{xy}\eta_{xy}\sigma_{\chi} + \tilde{\lambda}_{xx}(\eta_{xx} - \eta_{yy})\sigma_{\chi}$	$\lambda_{xy}k_xk_y\sigma_{\chi} + \lambda_{xx}(k_xk_x - k_yk_y)\sigma_{\chi}$ [45]
$\bar{1}\bar{4}\bar{1}2^{\infty}1$	$\tilde{\lambda}_{xy}\eta_{xy}\sigma_{\chi}$	$\lambda_{xy}k_xk_y\sigma_{\chi}$
$\bar{1}4\bar{1}m^1m^{\infty}1$	$\tilde{\lambda}_{xy}\eta_{xy}\sigma_{\chi}$	$\lambda_{xy}k_xk_y\sigma_{\chi}$
$\bar{1}\bar{4}\bar{1}2^1m^{\infty}1$	$\tilde{\lambda}_{xy}\eta_{xy}\sigma_{\chi}$	$\lambda_{xy}k_xk_y\sigma_{\chi}$
$\bar{1}\bar{4}\bar{1}m^12^{\infty}1$	$\tilde{\lambda}_{xy}\eta_{xy}\sigma_{\chi}$	$\lambda_{xy}k_xk_y\sigma_{\chi}$
$\bar{1}4/1m^{\bar{1}}m^1m^{\infty}1$	$\tilde{\lambda}_{xy}\eta_{xy}\sigma_{\chi}$	$\lambda_{xy}k_xk_y\sigma_{\chi}$ [37, 45]

collinear magnets, the spin-only group can be expressed as

$$G_{so} = \{U_{\parallel}(\phi)|1\} \oplus \{\mathcal{T}U_{\parallel}(\phi)U_{\perp}(\pi)|1\}, \quad (4)$$

where $U_{\parallel}(\phi)$ ($U_{\perp}(\pi)$) is spin rotation operation along the axis parallel (perpendicular) to χ , ϕ and π characterize the rotation angle, \mathcal{T} denotes the time-reversal operation, and 1 represents the identity spatial operation. As a matter of fact, the symmetry operations in G_{so} preserve both $\eta_{\alpha\beta}$ and σ_{χ} . Therefore, the G_{so} are not considered in our following symmetry analysis.

For each SPG, we shall work with its nontrivial spin point group G_{ns} and generate the symmetry-adapted $\hat{H}_{\text{eff}}(\{\eta_{\alpha,\beta}\}) = \sum_{\alpha\beta} \tilde{\lambda}_{\alpha\beta}\eta_{\alpha\beta}\sigma_{\chi}$ effective Hamiltonian by the projection operator technique (see e.g., Refs. [74, 75]). The effective Hamiltonian must be invariant with respect to the symmetry operations in G_{ns} . Therefore, the projection operator is defined according to the identity representation of the G_{ns} group, given by

$$\hat{\Pi} = \frac{1}{n(G_{ns})} \sum_{g \in G_{ns}} \hat{P}_g, \quad (5)$$

with $n(G_{ns})$ being the order of the G_{ns} group and \hat{P}_g being the symmetry operation in G_{ns} . We use the $\bar{1}4^{\infty}1$ SPG to demonstrate our procedures. The G_{ns} group for the $\bar{1}4^{\infty}1$ SPG contains four symmetry operations, and the effects of these operations on the $\eta_{\alpha\beta}$ strain and the σ_{χ} are shown in Table I. To derive the $\tilde{\lambda}_{\alpha\beta}\eta_{\alpha\beta}\sigma_{\chi}$ [see

Eq. (2)] for $\bar{1}4^{\infty}1$, we set up the projection operator as

$$\hat{\Pi} = \frac{1}{4}(P_{[1||1]} + P_{[1||2\circ\circ 1]} + P_{[\mathcal{T}||4\circ\circ 1]} + P_{[\mathcal{T}||4\bar{\circ}\circ 1]}),$$

and work with $\eta_{xx}\sigma_{\chi}$, $\eta_{yy}\sigma_{\chi}$, $\eta_{zz}\sigma_{\chi}$, $\eta_{xy}\sigma_{\chi}$, $\eta_{xz}\sigma_{\chi}$, and $\eta_{yz}\sigma_{\chi}$ as follows

- Case (i):

$$\begin{aligned} \hat{\Pi}\eta_{xx}\sigma_{\chi} &= \frac{1}{4}(\eta_{xx}\sigma_{\chi} + \eta_{xx}\sigma_{\chi} - \eta_{yy}\sigma_{\chi} - \eta_{yy}\sigma_{\chi}) \\ &= \frac{1}{2}(\eta_{xx} - \eta_{yy})\sigma_{\chi}, \end{aligned}$$

- Case (ii):

$$\begin{aligned} \hat{\Pi}\eta_{yy}\sigma_{\chi} &= \frac{1}{4}(\eta_{yy}\sigma_{\chi} + \eta_{yy}\sigma_{\chi} - \eta_{xx}\sigma_{\chi} - \eta_{xx}\sigma_{\chi}) \\ &= \frac{1}{2}(\eta_{yy} - \eta_{xx})\sigma_{\chi}, \end{aligned}$$

- Case (iii):

$$\begin{aligned} \hat{\Pi}\eta_{zz}\sigma_{\chi} &= \frac{1}{4}(\eta_{zz}\sigma_{\chi} + \eta_{zz}\sigma_{\chi} - \eta_{zz}\sigma_{\chi} - \eta_{zz}\sigma_{\chi}) \\ &= 0, \end{aligned}$$

- Case (iv):

$$\begin{aligned} \hat{\Pi}\eta_{xy}\sigma_{\chi} &= \frac{1}{4}(\eta_{xy}\sigma_{\chi} + \eta_{xy}\sigma_{\chi} + \eta_{xy}\sigma_{\chi} + \eta_{xy}\sigma_{\chi}) \\ &= \eta_{xy}\sigma_{\chi}, \end{aligned}$$

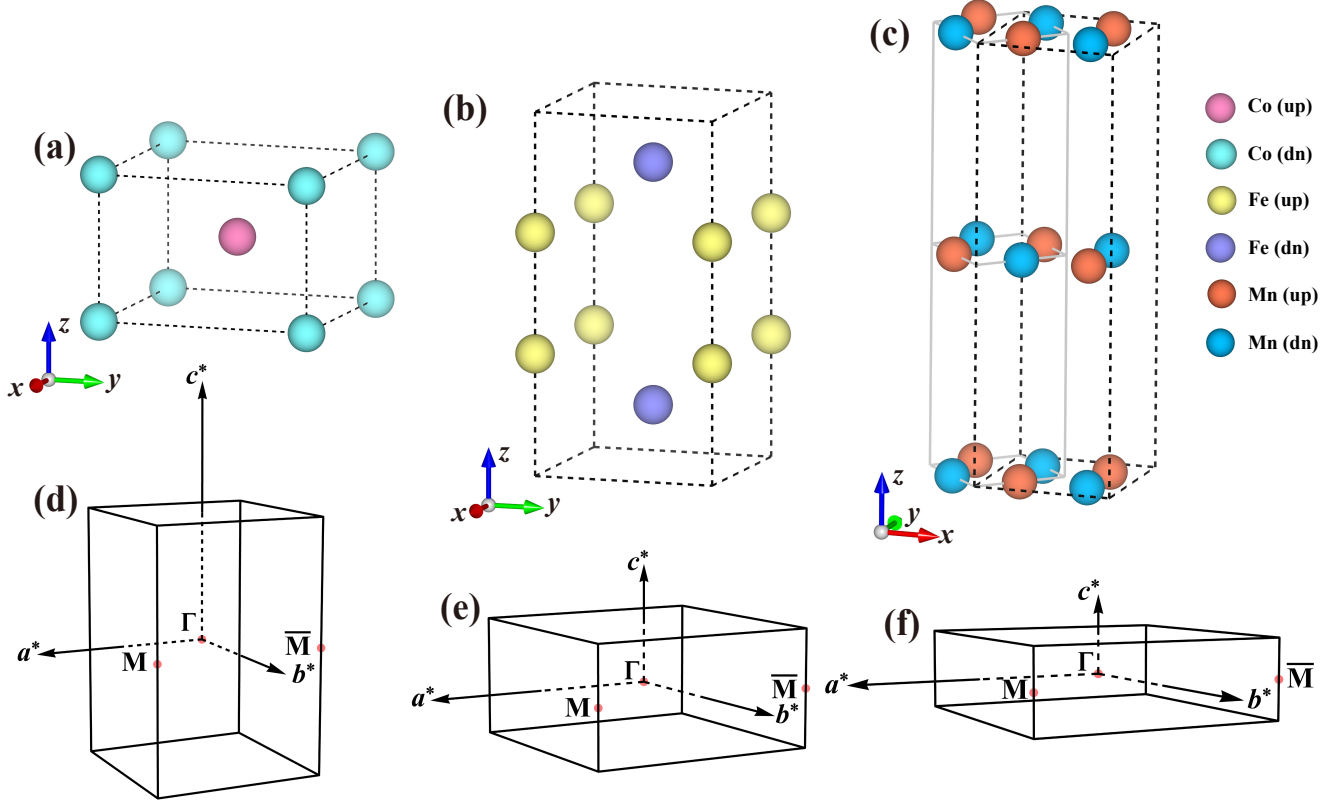


FIG. 2. Panels (a), (b), and (c) sketch the collinear magnetic structures for CoF_2 , LiFe_2F_6 , and $\text{La}_2\text{O}_3\text{Mn}_2\text{Se}_2$, respectively. The non-magnetic F, Li, La, Se and O ions are not displayed. Panels (d), (e), and (f) sketch the Brillouin zones for CoF_2 , LiFe_2F_6 , and $\text{La}_2\text{O}_3\text{Mn}_2\text{Se}_2$, respectively. The black dashed boxes in panels (a), (b), and (c) demonstrate the cells that are used in our simulations, while the grey solid box in panel (c) represents the conventional unit cell that is employed in literature (see e.g., Ref. [52]).

- Case (v):

$$\begin{aligned}\hat{\Pi}\eta_{xz}\sigma_\chi &= \frac{1}{4}(\eta_{xz}\sigma_\chi - \eta_{xz}\sigma_\chi - \eta_{yz}\sigma_\chi + \eta_{yz}\sigma_\chi) \\ &= 0,\end{aligned}$$

- Case (vi):

$$\begin{aligned}\hat{\Pi}\eta_{yz}\sigma_\chi &= \frac{1}{4}(\eta_{yz}\sigma_\chi - \eta_{yz}\sigma_\chi + \eta_{xz}\sigma_\chi - \eta_{xz}\sigma_\chi) \\ &= 0.\end{aligned}$$

The aforementioned results indicate that $\eta_{zz}\sigma_\chi$, $\eta_{xz}\sigma_\chi$, and $\eta_{yz}\sigma_\chi$ couplings are not symmetrically allowed in the $\bar{1}4^\infty m1$ SPG. In contrast, $\eta_{xx}\sigma_\chi$, $\eta_{yy}\sigma_\chi$, and $\eta_{xy}\sigma_\chi$ are allowed by symmetry. Here, cases (i) and (ii) suggest the $\tilde{\lambda}_{xx}(\eta_{xx} - \eta_{yy})\sigma_\chi$ coupling, while case (iv) implies the $\tilde{\lambda}_{xy}\eta_{xy}\sigma_\chi$ coupling. Overall, the effective Hamiltonian for the $\bar{1}4^\infty m1$ SPG is derived as $\tilde{H}_{\text{eff}}(\bar{1}4^\infty m1) = \tilde{\lambda}_{xx}(\eta_{xx} - \eta_{yy})\sigma_\chi + \tilde{\lambda}_{xy}\eta_{xy}\sigma_\chi$.

Similarly, we work with the 58 SPGs for collinear anti-ferromagnets and derive the effective Hamiltonians associated with strain-induced nonrelativistic ZSSs for these groups. We identify 15 SPGs that are compatible with strain-induced nonrelativistic ZSSs (see Table II). As shown in Ref. [37], these 15 SPGs belong to the category of *d*-wave altermagnetism. In Table II, we also derive the $\lambda_{\alpha\beta}k_\alpha k_\beta \sigma_\chi$ -type effective Hamiltonians that are associated with the alternating spin splittings; our derived Hamiltonians coincide with those shown in Refs. [37, 45]. Note that, the symbols marking the SPGs in our work are different from those in Ref. [37]. The symbols in Table II follow the conventions demonstrated in Refs. [68, 70–73].

B. *d*-wave altermagnets with strain-induced nonrelativistic ZSSs

We now verify our aforementioned theory by working with several typical *d*-wave altermagnets. According to Refs. [52, 76, 77], CoF_2 , LiFe_2F_6 , and $\text{La}_2\text{O}_3\text{Mn}_2\text{Se}_2$ are

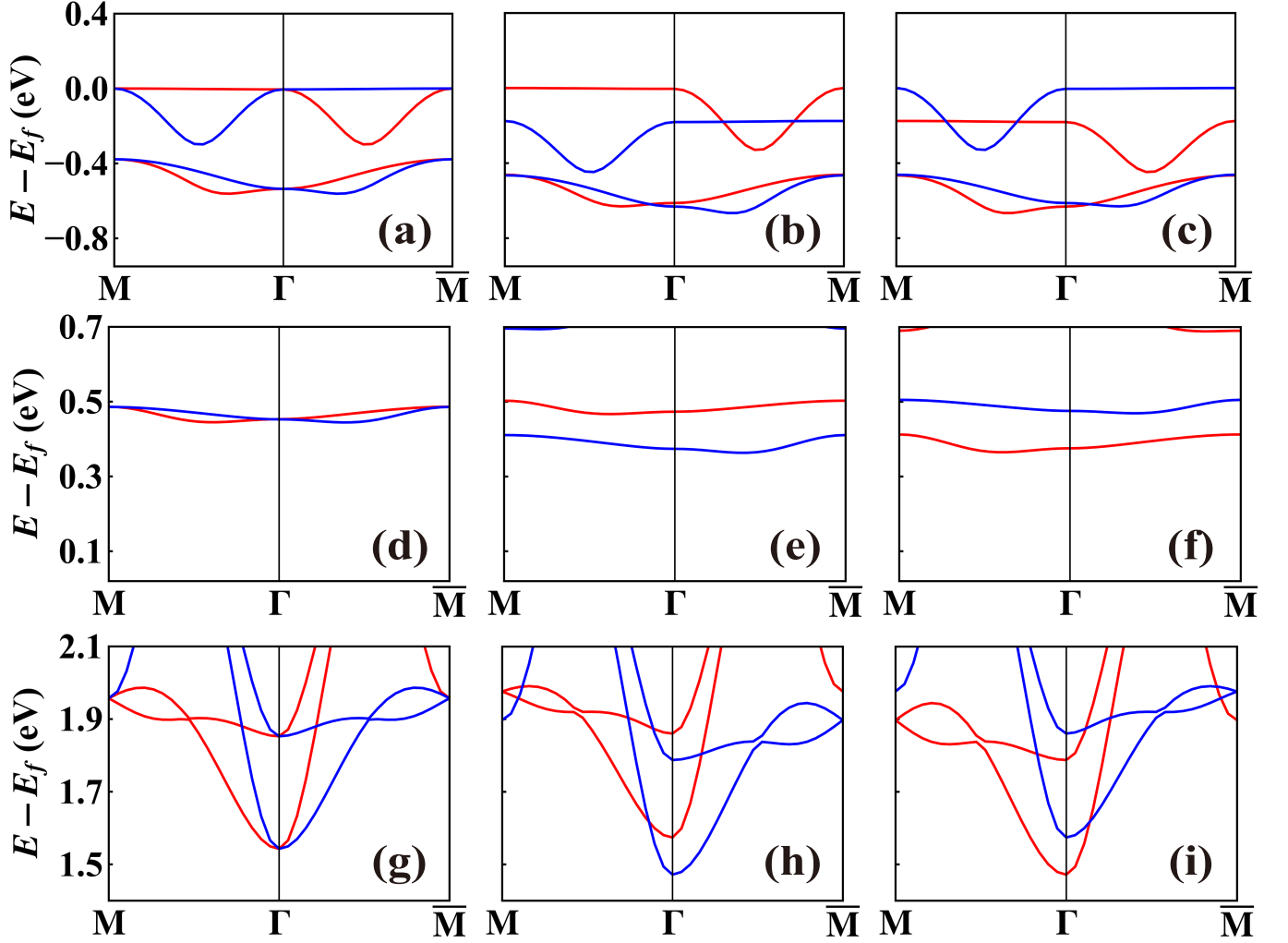


FIG. 3. The band structures along $M - \Gamma - \bar{M}$ high-symmetry lines for CoF_2 [(a), (b), and (c)], LiFe_2F_6 [(d), (e), and (f)], and $\text{La}_2\text{O}_3\text{Mn}_2\text{Se}_2$ [(g), (h), and (i)]. Panels (a), (d), and (g) are the band structures for the bulk materials without strain; Panels (b), (e), and (h) [respectively, (c), (f), and (i)] are the band structures for the strained materials with shear strain η_{xy} of +2% [respectively, -2%]. The spin-up and spin-down electronic states are colored in red and blue, respectively. The E_f level is set as the top of the valence band.

d -wave altermagnetic semiconductors that might showcase strain-induced nonrelativistic ZSSs. Experimentally, CoF_2 is an antiferromagnet with $P4_2/mnm$ crystallographic space group and $P4'_2/mnm'$ magnetic space group [78]. Figs. 2(a) and (d) show the collinear magnetic structure and the Brillouin zone for bulk CoF_2 . By the Find Spin Group code [68], we identify the spin point group of bulk CoF_2 as $\bar{1}4_1/m^1m^1m^\infty m1$. As shown in Table II, such a spin point group enables the η_{xy} -induced nonrelativistic ZSSs described by the effective Hamiltonian $\hat{\lambda}_{xy}\eta_{xy}\sigma_\chi$. This is verified by the band structures around the Γ point (calculated by first-principles) for CoF_2 . In Figs. 3(a), (b), and (c), we show the band structures (valence bands) for bulk CoF_2 and η_{xy} -strained CoF_2 . Without shear strain η_{xy} , the spin-up and spin-down energy levels at the Γ point are degenerate. The shear strain of $\pm 2\%$ creates nonrelativistic ZSSs

and modifies the band structures near the Γ point, where switching η_{xy} between +2% and -2% switches the spin feature of the electronic bands in CoF_2 .

Other examples are the d -wave altermagnetic LiFe_2F_6 and $\text{La}_2\text{O}_3\text{Mn}_2\text{Se}_2$ materials. Figs. 2(b), (c), (e), and (f) sketch the magnetic structures and Brillouin zones for bulk LiFe_2F_6 and $\text{La}_2\text{O}_3\text{Mn}_2\text{Se}_2$. Early experiment shows that LiFe_2F_6 has a space group of $P4_2/mnm$ [79]. Recent calculations and experiments suggest that LiFe_2F_6 is possibly multiferroic with a polar crystallographic space group of $P4_2nm$ [80] and a polar magnetic space group of $P4'_2nm'$ [54]. The spin point group of the polar LiFe_2F_6 is identified (by the Find Spin Group code [68]) as $\bar{1}4_1/m^1m^1m^\infty m1$. As for $\text{La}_2\text{O}_3\text{Mn}_2\text{Se}_2$, the crystallographic space group, magnetic space group, and spin point group (identified by the Find Spin Group code [68]) are $I4/mmm$, $I4'/mmm'$,

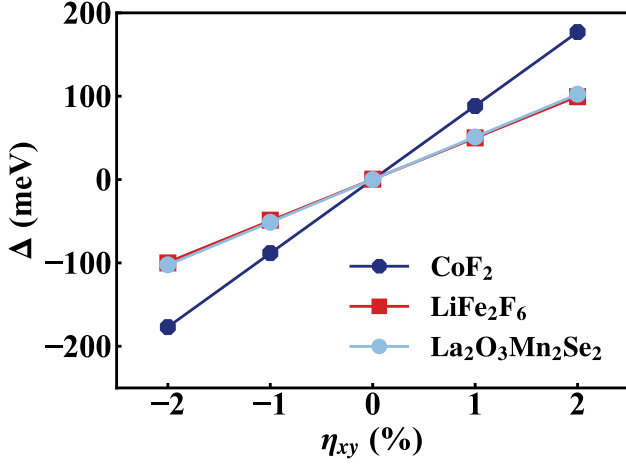


FIG. 4. The nonrelativistic ZSSs for CoF₂, LiFe₂F₆, and La₂O₃Mn₂Se₂ induced by shear strain η_{xy} . The ZSSs are extracted at the Γ point for CoF₂ (the two highest occupied valence bands), and at the Γ point LiFe₂F₆ and La₂O₃Mn₂Se₂ (the two lowest unoccupied conduction bands).

and $\bar{1}4/1m\bar{1}m^1m^\infty 1$, respectively [52]. Similar to CoF₂, both LiFe₂F₆ and La₂O₃Mn₂Se₂ host η_{xy} -induced nonrelativistic ZSSs as well, described by the effective Hamiltonian $\tilde{\lambda}_{xy}\eta_{xy}\sigma_\chi$ (see Table II). As shown in Figs. 3(d)–(i), our first-principles band structure calculations again confirm our analysis.

In Fig. 4, we show the nonrelativistic ZSSs (denoted by Δ) for CoF₂, LiFe₂F₆ and La₂O₃Mn₂Se₂ as functions of shear strain η_{xy} . As predicted by our theory (see $\tilde{H}_{\text{eff}}(\bar{1}4/1m\bar{1}m^1m^\infty 1) = \tilde{H}_{\text{eff}}(\bar{1}4\bar{1}m^1m^\infty 1) = \tilde{\lambda}_{xy}\eta_{xy}\sigma_\chi$ in Table II), the Δ splitting magnitude depends on η_{xy} linearly. More strikingly is that a shear strain of $\pm 2\%$ can induce giant nonrelativistic ZSSs as large as 177 meV, 100 meV, 102 meV for CoF₂, LiFe₂F₆ and

La₂O₃Mn₂Se₂.

IV. SUMMARY AND OUTLOOK

Based on symmetry arguments, we propose that d -wave altermagnets with $\lambda_{\alpha\beta}k_\alpha k_\beta \sigma_\chi$ altermagnetic spin splittings should host strain-induced nonrelativistic ZSSs (described by $\tilde{\lambda}_{\alpha\beta}\eta_{\alpha\beta}\sigma_\chi$) as well. We demonstrate that 15 collinear SPGs host strain-induced nonrelativistic ZSSs, where these SPGs coincide with the 15 cases hosting d -wave altermagnetic spin splittings (see Ref. [37]). The two-band effective models describing these two types of spin splittings are summarized in Table II. By first-principles simulations, we show that η_{xy} shear strain of 2% creates sizable ZSSs up to 177, 100, and 102 meV in CoF₂, LiFe₂F₆ and La₂O₃Mn₂Se₂ d -wave altermagnetic semiconductors, respectively. Compared with altermagnetic spin splittings, ZSSs offer another route towards the generation of spin current in antiferromagnets [4, 11, 81, 82]. As an outlook, our work implies that strain-induced ZSSs in d -wave altermagnets can be utilized to design altermagnetic-based spintronic devices.

V. ACKNOWLEDGEMENT

This work is supported by the National Key Research and Development Program of China (Grants No. 2023YFA1406103 and No. 2024YFA1409904) and the National Natural Science Foundation of China (Grants No. 12374005 and No. 12274174). Y. Z. thanks the support from high-performance computing center of Jilin University. H. J. Z. thanks the support from “Xiaomi YoungScholar” Project.

-
- [1] S. Wolf, D. Awschalom, R. Buhrman, J. Daughton, v. S. von Molnár, M. Roukes, A. Y. Chtchelkanova, and D. Treger, *Science* **294**, 1488 (2001).
 - [2] I. Žutić, J. Fabian, and S. D. Sarma, *Rev. Mod. Phys.* **76**, 323 (2004).
 - [3] P. Sharma, *Science* **307**, 531 (2005).
 - [4] S. Maekawa, S. O. Valenzuela, and E. Saitoh, *Spin current* (Oxford University Press, 2017).
 - [5] X. Liu, H. J. Zhao, L. Bellaiche, and Y. Ma, *Phys. Rev. B* **108**, 125108 (2023).
 - [6] M. Milivojević, M. Orozović, S. Picozzi, M. Gmitra, and S. Stavrčić, *2D Mater.* **11**, 035025 (2024).
 - [7] Y. Liu, J. Li, P. Liu, and Q. Liu, *Npj Quantum Mater.* **9**, 69 (2024).
 - [8] H. J. Zhao, X. Liu, Y. Wang, Y. Yang, L. Bellaiche, and Y. Ma, *Phys. Rev. Lett.* **129**, 187602 (2022).
 - [9] L. Tao, Q. Zhang, H. Li, H. J. Zhao, X. Wang, B. Song, E. Y. Tsybal, and L. Bellaiche, *Phys. Rev. Lett.* **133**, 096803 (2024).
 - [10] F. Lou, T. Gu, J. Ji, J. Feng, H. Xiang, and A. Stroppa, *Npj Comput. Mater.* **6**, 114 (2020).
 - [11] S. Maekawa, H. Adachi, K.-i. Uchida, J. Ieda, and E. Saitoh, *J. Phys. Soc. Jpn.* **82**, 102002 (2013).
 - [12] T. Schäpers, *Semiconductor spintronics* (Walter de Gruyter GmbH & Co KG, 2021).
 - [13] S. Hayami, Y. Yanagi, and H. Kusunose, *J. Phys. Soc. Jpn.* **88**, 123702 (2019).
 - [14] J. Krempaský, L. Šmejkal, S. D’souza, M. Hajlaoui, G. Springholz, K. Uhlířová, F. Alarab, P. Constantinou, V. Strocov, D. Usanov, *et al.*, *Nature* **626**, 517 (2024).
 - [15] S. Lee, S. Lee, S. Jung, J. Jung, D. Kim, Y. Lee, B. Seok, J. Kim, B. G. Park, L. Šmejkal, *et al.*, *Phys. Rev. Lett.* **132**, 036702 (2024).
 - [16] S. Reimers, L. Odenbreit, L. Šmejkal, V. N. Strocov, P. Constantinou, A. B. Hellenes, R. Jaeschke Ubierno, W. H. Campos, V. K. Bharadwaj, A. Chakraborty, *et al.*, *Nat. Commun.* **15**, 2116 (2024).

- [17] M. Hajlaoui, S. Wilfred D'Souza, L. Šmejkal, D. Krieger, G. Krizman, T. Zakusylo, N. Olszowska, O. Caha, J. Michalička, J. Sánchez-Barriga, *et al.*, *Adv. Mater.* **36**, 2314076 (2024).
- [18] M. Zeng, M.-Y. Zhu, Y.-P. Zhu, X.-R. Liu, X.-M. Ma, Y.-J. Hao, P. Liu, G. Qu, Y. Yang, Z. Jiang, *et al.*, *Adv. Sci.* **11**, 2406529 (2024).
- [19] G. Yang, Z. Li, S. Yang, J. Li, H. Zheng, W. Zhu, Z. Pan, Y. Xu, S. Cao, W. Zhao, *et al.*, *Nat. Commun.* **16**, 1442 (2025).
- [20] J. Ding, Z. Jiang, X. Chen, Z. Tao, Z. Liu, T. Li, J. Liu, J. Sun, J. Cheng, J. Liu, *et al.*, *Phys. Rev. Lett.* **133**, 206401 (2024).
- [21] O. Fedchenko, J. Minár, A. Akashdeep, S. W. D'Souza, D. Vasilyev, O. Tkach, L. Odenbreit, Q. Nguyen, D. Kutnyakhov, N. Wind, *et al.*, *Sci. Adv.* **10**, eadj4883 (2024).
- [22] L. Šmejkal, R. González-Hernández, T. Jungwirth, and J. Sinova, *Sci. Adv.* **6**, eaaz8809 (2020).
- [23] H. Reichlova, R. Lopes Seeger, R. González-Hernández, I. Kounta, R. Schlitz, D. Krieger, P. Ritzinger, M. Lamme, M. Leiviskä, A. Birk Hellenes, *et al.*, *Nat. Commun.* **15**, 4961 (2024).
- [24] Z. Feng, X. Zhou, L. Šmejkal, L. Wu, Z. Zhu, H. Guo, R. González-Hernández, X. Wang, H. Yan, P. Qin, *et al.*, *Nat. Electron.* **5**, 735 (2022).
- [25] R. Gonzalez Betancourt, J. Zubáč, R. Gonzalez-Hernandez, K. Geishendorf, Z. Šobán, G. Springholz, K. Olejník, L. Šmejkal, J. Sinova, T. Jungwirth, *et al.*, *Phys. Rev. Lett.* **130**, 036702 (2023).
- [26] L. Han, X. Fu, W. He, J. Dai, Y. Zhu, W. Yang, Y. Chen, J. Zhang, W. Zhu, H. Bai, *et al.*, *Phys. Rev. Appl.* **23**, 044066 (2025).
- [27] X. Zhou, W. Feng, R.-W. Zhang, L. Šmejkal, J. Sinova, Y. Mokrousov, and Y. Yao, *Phys. Rev. Lett.* **132**, 056701 (2024).
- [28] D.-F. Shao, S.-H. Zhang, M. Li, C.-B. Eom, and E. Y. Tsymbal, *Nat. Commun.* **12**, 7061 (2021).
- [29] D.-F. Shao and E. Y. Tsymbal, *Npj Spintron.* **2**, 13 (2024).
- [30] Y.-Y. Jiang, Z.-A. Wang, K. Samanta, S.-H. Zhang, R.-C. Xiao, W. Lu, Y. Sun, E. Y. Tsymbal, and D.-F. Shao, *Phys. Rev. B* **108**, 174439 (2023).
- [31] K. Samanta, D.-F. Shao, and E. Y. Tsymbal, *Nano Lett.* **25**, 3150 (2025).
- [32] L. Šmejkal, A. B. Hellenes, R. González-Hernández, J. Sinova, and T. Jungwirth, *Phys. Rev. X* **12**, 011028 (2022).
- [33] F. Liu, Z. Zhang, X. Yuan, Y. Liu, S. Zhu, Z. Lu, and R. Xiong, *Phys. Rev. B* **110**, 134437 (2024).
- [34] V. Baltz, A. Manchon, M. Tsoi, T. Moriyama, T. Ono, and Y. Tserkovnyak, *Rev. Mod. Phys.* **90**, 015005 (2018).
- [35] T. Jungwirth, X. Marti, P. Wadley, and J. Wunderlich, *Nat. Nanotechnol.* **11**, 231 (2016).
- [36] T. Jungwirth, J. Sinova, A. Manchon, X. Marti, J. Wunderlich, and C. Felser, *Nat. Phys.* **14**, 200 (2018).
- [37] L. Šmejkal, J. Sinova, and T. Jungwirth, *Phys. Rev. X* **12**, 031042 (2022).
- [38] R. González-Hernández, L. Šmejkal, K. Vybörny, Y. Yahagi, J. Sinova, T. Jungwirth, and J. Železný, *Phys. Rev. Lett.* **126**, 127701 (2021).
- [39] A. Bose, N. J. Schreiber, R. Jain, D.-F. Shao, H. P. Nair, J. Sun, X. S. Zhang, D. A. Muller, E. Y. Tsymbal, D. G. Schlom, *et al.*, *Nat. Electron.* **5**, 267 (2022).
- [40] H. Bai, L. Han, X. Feng, Y. Zhou, R. Su, Q. Wang, L. Liao, W. Zhu, X. Chen, F. Pan, *et al.*, *Phys. Rev. Lett.* **128**, 197202 (2022).
- [41] S. Karube, T. Tanaka, D. Sugawara, N. Kadoguchi, M. Kohda, and J. Nitta, *Phys. Rev. Lett.* **129**, 137201 (2022).
- [42] M. Naka, S. Hayami, H. Kusunose, Y. Yanagi, Y. Motome, and H. Seo, *Nat. Commun.* **10**, 4305 (2019).
- [43] M. Naka, Y. Motome, and H. Seo, *Phys. Rev. B* **103**, 125114 (2021).
- [44] M. Ezawa, *Phys. Rev. B* **111**, 125420 (2025).
- [45] M. Roig, A. Kreisel, Y. Yu, B. M. Andersen, and D. F. Agterberg, *Phys. Rev. B* **110**, 144412 (2024).
- [46] L. C. L. Y. Voon and M. Willatzen, *The kp method: electronic properties of semiconductors* (Springer Science & Business Media, 2009).
- [47] G. Kresse and J. Furthmüller, *Phys. Rev. B* **54**, 11169 (1996).
- [48] G. Kresse and D. Joubert, *Phys. Rev. B* **59**, 1758 (1999).
- [49] J. P. Perdew, K. Burke, and M. Ernzerhof, *Phys. Rev. Lett.* **77**, 3865 (1996).
- [50] P. E. Blöchl, *Phys. Rev. B* **50**, 17953 (1994).
- [51] S. L. Dudarev, G. A. Botton, S. Y. Savrasov, C. Humphreys, and A. P. Sutton, *Phys. Rev. B* **57**, 1505 (1998).
- [52] C.-C. Wei, X. Li, S. Hatt, X. Huai, J. Liu, B. Singh, K.-M. Kim, R. M. Fernandes, P. Cardon, L. Zhao, *et al.*, *Phys. Rev. Mater.* **9**, 024402 (2025).
- [53] Q. Ma, B. Wang, G. Yang, and Y. Liu, *arXiv:2502.10055* (2025).
- [54] L.-F. Lin, Q.-R. Xu, Y. Zhang, J.-J. Zhang, Y.-P. Liang, and S. Dong, *Phys. Rev. Mater.* **1**, 071401 (2017).
- [55] V. Wang, N. Xu, J.-C. Liu, G. Tang, and W.-T. Geng, *Comput. Phys. Commun.* **267**, 108033 (2021).
- [56] VASPkit, <https://vaspkit.com>.
- [57] K. Momma and F. Izumi, *J Appl. Crystallogr.* **44**, 1272 (2011).
- [58] See, <https://www.wolfram.com/mathematica>.
- [59] M. I. Aroyo, J. M. Perez-Mato, D. Orobengoa, E. Tasci, G. de la Flor, and A. Kirov, *Bulg. Chem. Commun.* **43**, 183 (2011).
- [60] M. I. Aroyo, J. M. Perez-Mato, C. Capillas, E. Kroumova, S. Ivantchev, G. Madariaga, A. Kirov, and H. Wondratschek, *Z. Kristallogr. Cryst. Mater.* **221**, 15 (2006).
- [61] M. I. Aroyo, A. Kirov, C. Capillas, J. Perez-Mato, and H. Wondratschek, *Acta Crystallogr. Sect. A: Found. Crystallogr.* **62**, 115 (2006).
- [62] S. V. Gallego, J. M. Perez-Mato, L. Elcoro, E. S. Tasci, R. M. Hanson, K. Momma, M. I. Aroyo, and G. Madariaga, *Journal of Applied Crystallography* **49**, 1750 (2016).
- [63] S. V. Gallego, J. M. Perez-Mato, L. Elcoro, E. S. Tasci, R. M. Hanson, M. I. Aroyo, and G. Madariaga, *J. Appl. Crystallogr.* **49**, 1941 (2016).
- [64] Magndata, <http://webbdcristal.ehu.es/magndata>.
- [65] U. Herath, P. Tavadze, X. He, E. Bousquet, S. Singh, F. Muñoz, and A. H. Romero, *Comput. Phys. Commun.* **251**, 107080 (2020).
- [66] Pyprocar, <https://romerogroup.github.io/pyprocar/index.html>.
- [67] A. Jain, S. P. Ong, G. Hautier, W. Chen, W. D. Richards, S. Dacek, S. Cholia, D. Gunter, D. Skinner, G. Ceder, *et al.*, *APL Mater.* **1**, 011002 (2013).

- [68] X. Chen, J. Ren, Y. Zhu, Y. Yu, A. Zhang, P. Liu, J. Li, Y. Liu, C. Li, and Q. Liu, [Phys. Rev. X. **14**, 031038 \(2024\)](#).
- [69] J. D. Hunter, [Comput. Sci. Eng. **9**, 90 \(2007\)](#).
- [70] D. B. Litvin and W. Opechowski, [Physica **76**, 538 \(1974\)](#).
- [71] D. B. Litvin, [Acta Crystallogr. Sect. A: Found. Crystallogr. **33**, 279 \(1977\)](#).
- [72] P. Liu, J. Li, J. Han, X. Wan, and Q. Liu, [Phys. Rev. X **12**, 021016 \(2022\)](#).
- [73] H. Schiff, A. Corticelli, A. Guerreiro, J. Romhányi, and P. A. McClarty, [SciPost Phys. **18**, 109 \(2025\)](#).
- [74] M. S. Dresselhaus, G. Dresselhaus, and A. Jorio, [Group theory: application to the physics of condensed matter](#) (Springer Science & Business Media, 2007).
- [75] R. M. Geilhufe and W. Hergert, [Front. Phys. **6**, 86 \(2018\)](#).
- [76] P.-J. Guo, Y. Gu, Z.-F. Gao, and Z.-Y. Lu, [arXiv:2312.13911 \(2023\)](#).
- [77] Y. Guo, H. Liu, O. Janson, I. C. Fulga, J. van den Brink, and J. I. Facio, [Mater. Today Phys. **32**, 100991 \(2023\)](#).
- [78] J. Strempfer, U. Rütt, S. Bayrakci, T. Brückel, and W. Jauch, [Phys. Rev. B **69**, 014417 \(2004\)](#).
- [79] G. Shachar, J. Makovsky, and H. Shaked, [Phys. Rev. B **6**, 1968 \(1972\)](#).
- [80] J. Fourquet, E. Le Samedi, and Y. Calage, [J. Solid State Chem. **77**, 84 \(1988\)](#).
- [81] D. C. Ralph and M. D. Stiles, [J. Magn. Magn. Mater. **320**, 1190 \(2008\)](#).
- [82] A. Brataas, A. D. Kent, and H. Ohno, [Nat. Mater. **11**, 372 \(2012\)](#).